

## Validation and Comparison of Patient-Specific SAR Models

H. Homann<sup>1</sup>, P. Börnert<sup>2</sup>, K. Nehrke<sup>2</sup>, H. Eggers<sup>2</sup>, O. Dössel<sup>1</sup>, and I. Graesslin<sup>2</sup>

<sup>1</sup>Institute of Biomedical Engineering, Karlsruhe Institute of Technology, Karlsruhe, Germany, <sup>2</sup>Philips Research Europe, Hamburg, Germany

### Introduction

The specific absorption rate (SAR) is an important safety criterion in high-field MRI ( $\geq 3T$ ). In the sequence design, the SAR often limits the allowed flip-angle or repetition time and hence contrast as well as total scan time. SAR simulations for generic body models are typically performed to assess patient safety. However, the local SAR hotspots are patient-dependent [1] and hence there is an intrinsic uncertainty in such simulations.

In a previous study [2], a novel approach for generating patient-specific models based on water-fat-separated MR data was proposed. This was motivated by the fact that the eddy current paths inside the body are mostly determined by the water-fat distribution [3]. In this study, the simulated RF fields are validated for different regions of the human body by *in vivo* B1-mapping to gain more confidence in SAR simulations. Furthermore, the SAR distributions in several volunteers are compared for a better understanding of SAR hotspot formation.

### Methods

Whole-body chemical-shift encoded 3D MR scans were performed on 5 volunteers (age 29-43years, weight 65-86kg) using an isotropic spatial resolution of 5mm. Imaging was performed on a 3T MR scanner (Philips Healthcare, Best, The Netherlands), equipped with a parallel transmit body coil with 8 TEM elements [4]. All elements were calibrated to equal current amplitude and quadrature phases.

B1-maps were acquired directly after the whole-body scans in the same body pose for different anatomical planes and at different anatomical regions (head, abdomen, legs). For efficient B1-mapping within a single breathhold, the actual flip angle (AFI) sequence [5] was applied ( $5 \times 5 \times 15 \text{ mm}^3$  voxel size,  $\text{TR}_1/\text{TR}_2: 20/100 \text{ ms}$ ,  $\alpha = 50^\circ$ ).

For segmentation of the whole-body data into regions dominated by water or fat, a three-point Dixon approach [6] was applied. The lungs were identified by region-growing. Dielectric properties according to [7] were assigned to the water, fat, and lung segments, where the properties of muscle were chosen to represent all water-rich tissues. The resulting segmented models were placed inside a model of the RF body coil in the same orientation and position as used for the B1-mapping scans. Finite-differences time-domain (FDTD) simulations were carried out using a commercial solver (XFDTD, Remcom Inc., PA, USA) for each TX element independently. The simulation results were post-processed to achieve the same current-distribution in all TX-elements of the body coil as in the B1-mapping scans. Electric and magnetic fields were scaled for an MR sequence with a root-mean-square of  $B1_{\text{rms}} = 1 \mu\text{T}$ . The local 10g-averaged and the global SAR were calculated. The simulated B1-fields were validated against the measured B1-maps.

### Results and Discussion

Simulated and measured B1-field maps are compared for a selected volunteer in Fig. 1. The general field pattern in the simulation agrees well with the measurements, indicating that the RF wave propagation in different parts of the human body is reasonably represented by the simulation. Quantitative agreement is also obtained, the standard deviations of the difference images range from 14.2% to 26.8%. Though the electric field cannot be measured directly, it is coupled to the magnetic field via Maxwell's equations. Hence, the error can be expected to be in the same order of magnitude.

The global SAR values ranged from 0.37 to 0.59W/kg. The local SAR values vary significantly between the volunteers (cf. Fig 2). However, all volunteers showed similar hotspots of the local SAR, occurring at narrow regions of the muscles at the pelvis and at the shoulders. Relatively high SAR values occurred in the arms when stretched out beside the body in parallel to the TEM coil elements due to increased RF coupling. The SAR level in the arms of volunteer 2 drastically reduced when moving the arms onto the body, but not touching the body in order to avoid a current loop.

### Conclusions

The use of water-fat-separated MR data is a relatively simple and flexible approach for generating dielectric body models. Whereas most generic models are more detailed, to our knowledge no *in vivo* validation of such models has ever been performed. In this study, good agreement between the measured and the simulated B1-fields was found, suggesting that the water-fat-separated models accurately represent the eddy current paths through the human body and hence also give a valid estimation of the SAR.

The approach can in principle be used for patient-specific SAR model generation. Such models may be valuable for research in high-field MRI or for *in vivo* validation RF coil simulations. For a clinical application, this is currently not practical. Instead, the approach can be used to generate models representing various anatomies and body positions for comparative studies of the SAR. The models used in this work exhibit very consistent local SAR patterns. This provides further confidence in the reliability of the SAR prediction and motivates further research in SAR management and local SAR hotspot suppression by parallel transmit MRI.

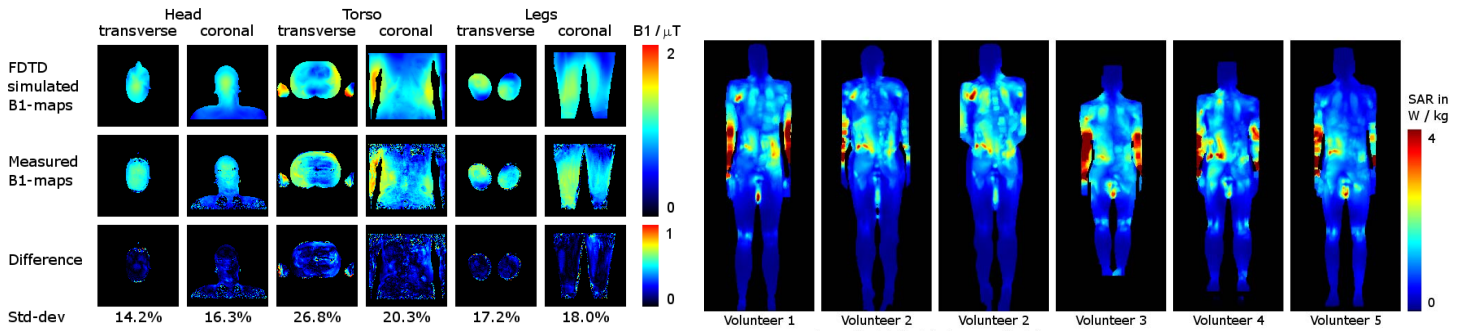


**Fig. 1:** Comparison of measured and simulated B1-fields in one volunteer at three different locations in the MR scanner.

**Fig. 2:** Maximum intensity projections of the 10g-averaged local SAR for the five volunteers, showing similar SAR hotspots inside all bodies.

**References** [1] C.M.Collins MRM 40:847-856 (1998) [2] H.Homann, Proc. ISMRM 2010:3874 [3] H.Homann, Proc. ESMRMB 2009:195 [4] P.Vernickel, MRM 58:381-389 (2007) [5] S.B.Reeder, MRM 51:34-45 (2004) [6] V.L.Yarnykh, MRM 57:192-200 (2007) [7] S.Gabriel, PMB 41:2231-2293 (1996)